

Article

# Transient Tests for Checking the Trieste Subsea Pipeline: Diving into Fault Detection

Silvia Meniconi <sup>1</sup> , Bruno Brunone <sup>1</sup> , Lorenzo Tirello <sup>2</sup>, Andrea Rubin <sup>2</sup>, Marco Cifrodelli <sup>3</sup>   
and Caterina Capponi <sup>1,\*</sup> 

<sup>1</sup> Department of Civil and Environmental Engineering, The University of Perugia, 06125 Perugia, Italy; silvia.meniconi@unipg.it (S.M.); bruno.brunone@unipg.it (B.B.)

<sup>2</sup> AcegasApsAmga SpA, 35128 Padova, Italy; ltirello@acegasapsamga.it (L.T.); arubin@acegasapsamga.it (A.R.)

<sup>3</sup> Umbria Regional Forestry Agency, 06036 Perugia, Italy; marco.cifrodelli.pg@gmail.com

\* Correspondence: caterina.capponi@unipg.it

**Abstract:** Fault detection in subsea pipelines is a difficult problem for several reasons, and one of the most important is the inaccessibility of the system. This criticality can be overcome by using transient test-based techniques. Such an approach is based on the execution of safe transients that result in small over pressures (i.e., on the order of a few meters of water column). In our companion paper, the procedure involving the transient tests was described in detail. This paper analyses the results of the field tests carried out and identifies wall deterioration in some sections of the pipeline. Attention is focused on the numerical procedure based on the joint use of a 1-D numerical model simulating transients in the pressurized flow and analytical relationships and providing the transient response of anomalies such as leaks and wall deterioration. The results obtained are essentially confirmed by the survey carried out by divers.

**Keywords:** subsea pipeline; fault detection; transient test; anomaly transient response; wall deterioration



**Citation:** Meniconi, S.; Brunone, B.; Tirello, L.; Rubin, A.; Cifrodelli, M.; Capponi, C. Transient Tests for Checking the Trieste Subsea Pipeline: Diving into Fault Detection. *J. Mar. Sci. Eng.* **2024**, *12*, 391. <https://doi.org/10.3390/jmse12030391>

Academic Editor: Dejan Brkić

Received: 8 January 2024

Revised: 19 February 2024

Accepted: 21 February 2024

Published: 24 February 2024



**Copyright:** © 2024 by the authors. Licensee MDPI, Basel, Switzerland. This article is an open access article distributed under the terms and conditions of the Creative Commons Attribution (CC BY) license (<https://creativecommons.org/licenses/by/4.0/>).

## 1. Introduction

Recent developments in water resource management have recognized the critical importance of addressing fault detection in long transmission mains [1]. This is particularly vital for subsea pipelines (SPs), where leaks not only result in significant water loss but also pose environmental risks and challenges in maintenance due to their inaccessible underwater locations. Given that transmission mains, and then SPs, are responsible for transporting the entire volume of discharge, even minor leakage can result in significant water loss. Other anomalies, such as pipe wall deterioration, can cause the pipe to burst and then leak. Consequently, the need for advanced fault detection techniques has become increasingly evident for SPs.

In our companion paper [2], after highlighting the main issues related to fault detection in SPs, attention was focused on the Trieste (Italy) SP (Figure 1). According to the characteristics of the water supply system that includes the Trieste SP, the transient test-based techniques (TTBTs) have been identified as the most suitable approach for fault detection. As described in [2], historically, Smart Pigging, Acoustic Monitoring, Remotely Operated Vehicles, and diving constitute the foundational methods for pipeline inspection. Each of these techniques is marked by significant costs and certain limitations, e.g., [3–8]. In this perspective, the hydraulic characterization of the small-diameter side discharge valve (SDV) used to generate a safe transient was carried out. Successively, the appropriate procedure for performing reliable transient tests has been outlined. Precisely, the maneuvers preceding the transient test as well as the subsequent maneuvers were illustrated and motivated. The aim of the preliminary maneuvers was to bring the system to appropriate steady-state conditions. The aim of the subsequent maneuvers was to restore the normal

operating conditions. As mentioned in our companion paper [2], TTBTs are based on the analysis of the dynamics of transients in pressurized flows, in particular on the interaction of the pressure waves with the anomalies. Precisely, when pressure waves inserted into the pipeline encounter an anomaly, they are reflected partially back, allowing the anomaly to be identified and localized from the characteristics of the reflected pressure wave and its arrival time in the measurement sections. Figure 2 gives examples of the effect of different anomalies on the pressure signal,  $H$ , in a reservoir pipe valve (RPV) system. In particular, in the pressure signal acquired at the downstream end section of the RPV system where the transient is generated, the footprint of a leak (or branch) is a negative pressure wave [9–11],  $\Delta H_L^-$  (Figure 2a), whereas a partially closed in-line valve results in a positive pressure wave [12–16],  $\Delta H_V^+$  (Figure 2b). Extended partial blockage causes a positive wave,  $\Delta H_{BL}^+$ , followed by a negative one [17,18],  $\Delta H_{BL}^-$  (a sort of “positive bell”, Figure 2c), while partial wall deterioration causes a negative wave,  $\Delta H_{WD}^-$ , followed by a positive one,  $\Delta H_{WD}^+$  (a sort of “negative bell”, Figure 2d) [19]. The entity of the mentioned pressure variations depends strictly on the size of the anomaly. In the figure,  $\theta (= t/\tau)$  is the dimensionless time, where  $t$  is the time elapsed since the beginning of the transient, and  $\tau$ , the pipe characteristic time, is equal to  $2L/a$ , with  $L$  = pipe length, and  $a$  = pressure wave speed; the subscripts  $L$ ,  $V$ ,  $BL$ , and  $WD$  refer to quantities to leak, the in-line valve, extended partial blockage, and wall deterioration, respectively.

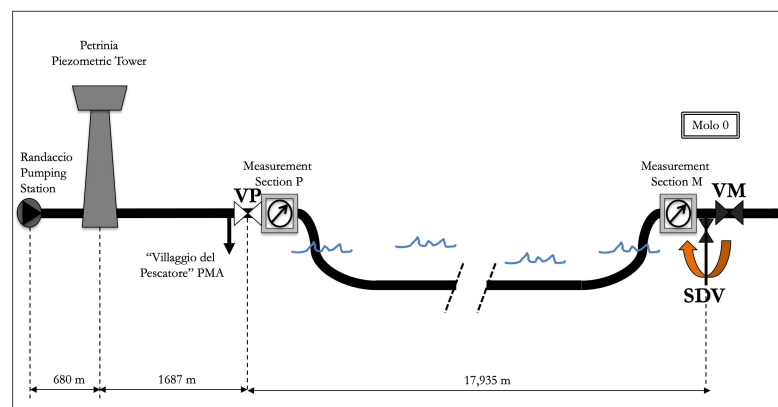


**Figure 1.** Sketch of the Trieste subsea pipeline (SP) (from [2]).

The literature contains various approaches for interpreting pressure signals, such as time- and frequency-domain direct analysis, inverse transient analysis (ITA), and wavelet analysis [20–26]. These methods are designed to maximize the information gained from transient tests on the condition of the pipe and provide a comprehensive understanding of its condition. In this paper, a transient numerical model is used within an ITA trial-and-error procedure in which the effect of the hypothesized anomalies is simulated and the results are then compared with the acquired pressure signal.

Preliminarily, it is crucial to acknowledge some of the limitations of TTBTs in providing a comprehensive assessment of pipeline condition, e.g., [27]. The complexity of analyzing a pressure pipe system escalates with its intricate topology, such as branches, connections, and end-users [28–30]. These elements introduce additional pressure waves, complicating the interpretation of the transient response of faults. Consequently, the pressure signal at any given section is the result of an overlapping of pressure waves originating from various elements, making the isolation of anomalies within this signal exceedingly challenging without extensive measurement points and precise knowledge of all boundary and initial conditions. Furthermore, the ambiguity of the pressure damping in the time-domain, as evidenced by numerical and laboratory experiments, adds another layer of complexity. In [31], it is demonstrated that different leak parameters can produce identical pressure damping effects. This underscores the fact that numerical simulations, aimed at mirroring the essential aspects of the transient response, cannot be expected to perfectly match

experimental signals. Such an exact alignment is not only unrealistic but also unnecessary from a management standpoint due to inevitable variances stemming from uncertainties in pipe physical properties (e.g., roughness), boundary conditions, and data noise.

To automate the analysis process, integrating machine learning methods with TTBTs appears promising [32–34]. However, achieving this requires assembling an extensive collection of transient pressure signal datasets from both numerical simulations and experimental trials, encompassing lab and field studies. This comprehensive dataset is essential for refining the accuracy and reliability of TTBTs when coupled with advanced analytical techniques.

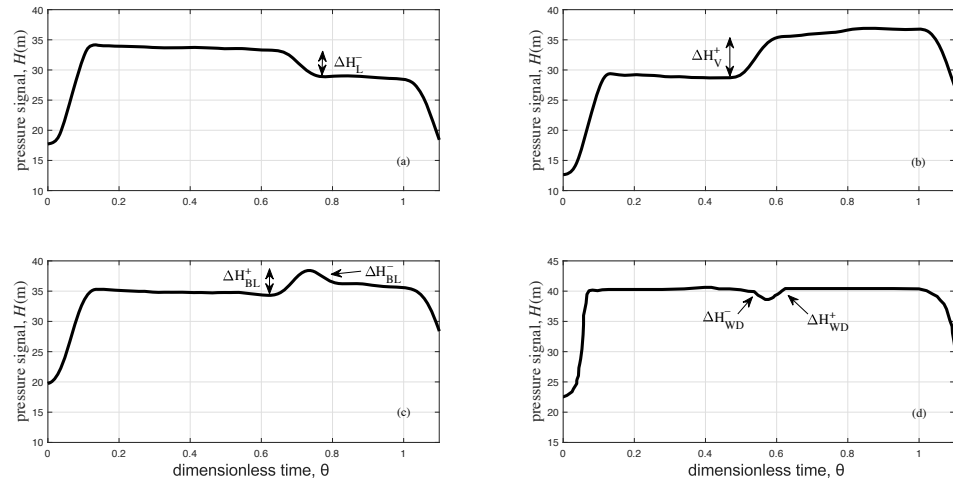


**Figure 2.** Reservoir pipe valve (RPV) system: anomaly effect in the pressure signal during the first characteristic time of the pipe: (a) leak or branch, e.g., [31]; (b) partially closed in-line valve, e.g., [16]; (c) extended partial blockage, e.g., [16]; and (d) wall deterioration (modified from [35]).

This paper shows the application of TTBTs to the Trieste SP with the aim of demonstrating the effectiveness of this methodology for fault detection. Accordingly, its structure is as follows: Section 2 introduces the numerical and analytical models used. Section 3 discusses the executed field tests. Section 4 shows the inverse transient procedure executed for detecting anomalies. Finally, the obtained results are synthesized in Section 5.

## 2. Materials and Methods

### 2.1. One-Dimensional Numerical Model

As detailed in [36–39], the 1-D numerical model is based on the differential equations governing transients in elastic pressurized pipelines:

$$\frac{\partial H}{\partial t} + \frac{a^2}{gA} \frac{\partial Q}{\partial s} = 0 \tag{1}$$

which is the continuity equation, and

$$\frac{\partial H}{\partial s} + \frac{1}{gA} \frac{\partial Q}{\partial t} + J_s + J_u = 0 \tag{2}$$

which is the momentum equation, where  $H$  = piezometric head,  $Q$  = discharge,  $s$  = axial coordinate,  $A$  = pipe cross-sectional area,  $g$  = acceleration of gravity, and  $J_s$  ( $J_u$ ) = steady-state (unsteady) friction term. Within the Allievi–Joukowsky approach, the pressure wave speed,  $a$ , can be evaluated as:

$$a = \sqrt{\frac{K}{\rho \left(1 + \frac{K D}{E e}\right)}} \tag{3}$$

where  $K$  = bulk modulus of the fluid,  $\rho$  = density of the fluid,  $E$  = Young’s modulus of the pipe material,  $D$  = internal pipe diameter, and  $e$  = pipe thickness.

The 1-D numerical model integrates Equations (1) and (2) using the Method of Characteristics (MOCs), a technique that solves hyperbolic partial differential equations by reducing them to ordinary differential equations along characteristic lines. In this model, each pipe, characterized by constant geometric properties, is subdivided into sections or reaches, of length  $\Delta s_j$ . This subdivision is defined such that  $\Delta s_j = a_j \Delta t$ , where  $\Delta t$  represents the time step, and the subscript  $j$  denotes the specific pipe. If suitable, in the simulations, the value of  $\Delta t$  can match the experimental time step used for pressure measurements, i.e.,  $\Delta t = 1/f_a$ , with  $f_a$  = data frequency acquisition. This alignment ensures consistency between the model and experimental observations.

Within the MOC framework, Equations (1) and (2) are reformulated into a set of algebraic compatibility equations for each internal computational node. These equations are:

$$C^+ : H_i^t = C_P - B_P Q_i^t \tag{4}$$

$$C^- : H_i^t = C_N + B_N Q_i^t \tag{5}$$

valid along the characteristic lines  $C^+$  and  $C^-$ , respectively, with the subscript  $i$  indicating the node and the superscript  $t$  the time step. The coefficients  $C_P$ ,  $C_N$ ,  $B_P$ , and  $B_N$  are determined based on the values of  $Q$  and  $H$  at the preceding time step. When the unsteady-state friction term,  $J_u$ , is modeled using an instantaneous acceleration-based approach, e.g., [40,41], the equations take the following forms:

$$C_P = H_{i-1}^{t-\Delta t} + B_j Q_{i-1}^{t-\Delta t} - k_B B_j [(Q_{i-1}^{t-\Delta t} - Q_{i-1}^{t-2\Delta t}) + \text{sign}(Q_i^{t-\Delta t}) |Q_i^{t-\Delta t} - Q_{i-1}^{t-\Delta t}|] \tag{6}$$

$$C_N = H_{i+1}^{t-\Delta t} - B_j Q_{i+1}^{t-\Delta t} + k_B B_j [(Q_{i+1}^{t-\Delta t} - Q_{i+1}^{t-2\Delta t}) + \text{sign}(Q_i^{t-\Delta t}) |Q_i^{t-\Delta t} - Q_{i+1}^{t-\Delta t}|] \tag{7}$$

$$B_P = B_j + R_j |Q_{i-1}^{t-\Delta t}| \tag{8}$$

$$B_N = B_j + R_j |Q_{i+1}^{t-\Delta t}| \tag{9}$$

In these equations, the coefficients  $k_B$ ,  $B_j$ , and  $R_j$  represent the unsteady-state decay coefficient [40,41], the characteristic impedance, and the pipe resistance coefficient, respectively. Due to its minimal impact during the initial phase of the transient (i.e., the first characteristic time of the pipeline), on which attention is focused for fault detection, it has been decided to neglect the unsteady-state friction term ( $k_B = 0$ ). This simplification does not affect the procedure and streamlines the model while maintaining accuracy for the focused transient phase.

### 2.2. Boundary Conditions

Firstly, at the Petrinia piezometric tower the model assumes a constant value of the piezometric head,  $H_T$ , as during the first characteristic time of the transient its variation is negligible.

Secondly, the model calibration involves determining the actual hydraulic behavior of the maneuver valve,  $A_E$ , and the duration of the maneuver,  $T$ , through ITA. The relationship between the discharge,  $Q_{SDV}$ , and the pressure head,  $H_{SDV}$ , at the downstream end of the pipe is given by [36]:

$$Q_{SDV}^t = \frac{Q^0 A_E^t \sqrt{H_{SDV}^t}}{\sqrt{H_{SDV}^t}} \tag{10}$$

In this equation,  $Q_{SDV}^t$  and the valve effective area,  $A_E^t$ , are the unknowns, while  $H_{SDV}^t$  is measured during the valve maneuver. The time at which  $Q_{SDV}$  equals zero corresponds to the value of  $T$ . This approach allows for accurate modeling of the valve’s characteristics, even if it is operated manually.

### 2.3. Analytical Model for Evaluating the Effect of the Anomalies

In the absence of in-line valves, only scenarios involving leaks and pipe wall deterioration are considered. As for the evaluation of the inserted pressure wave [2],  $\Delta H$ , a simplified analytical approach allows us to evaluate the transient response of these anomalies (Figure 2a,d).

For the leak, it results in a pressure reduction  $\Delta H_L^-$  [42]:

$$\Delta H_L^- = C_{R,L} \Delta H = \left( 1 + \frac{2AQ_L^0}{a(C_{L,d}A_L)^2} \right)^{-1} \Delta H = \left( 1 + \frac{2A\sqrt{2g(H_L^0 - z_L)}}{aA_{L,E}} \right)^{-1} \Delta H \quad (11)$$

where  $C_{R,L}$  = reflection coefficient at the leak,  $C_{L,d}$  = leak discharge coefficient,  $A_L$  = leak area, and  $A_{L,E}$  = leak effective area.

Wall deterioration encompasses either a reduced diameter section or a thinner wall thickness, leading to an increased internal diameter or a decrease in pipe thickness while maintaining a constant internal diameter. The initial pressure variation ( $\Delta H_j$ ), either  $\Delta H_j = \Delta H_{PB}^+$  for partial blockages or  $\Delta H_j = \Delta H_{PWD}^-$  for wall deterioration, is calculated as follows:

$$\Delta H_j = C_{R,j} \Delta H = \frac{A/a - A_j/a_j}{A/a + A_j/a_j} \Delta H \quad (12)$$

where  $C_{R,j}$  is the reflection coefficient.

### 3. Field Tests

Figure 3 presents the pressure signals,  $H$ , recorded at sections M and P during the sudden manual closure of the SDV; in this figure,  $t_5$  is the time at which the closure of the SDV started [2]. Notably,  $H_M$  exhibits (i) a steady-state value very close to the value previously indicated by the water supply manager's ( $H_{M,0} = 72.3$  m) and (ii) an increase of  $\Delta H_{M,1} = 0.53$  m due to the maneuver at  $t_{M,1} = 0$ . The pressure signal at section P displays a slightly lower increase  $\Delta H_{P,1} = 0.43$  m at  $t_{P,1} = 15.3$  s. In both sections, these first pressure variations are followed by oscillations that progressively dampen, settling into hydrostatic conditions after roughly 30 min.

It is worth noting that the variations in the pressure signal are analyzed using wavelet analysis to automatically evaluate the arrival time of pressure waves with high precision. This method decomposes the pressure signal into different frequency components, enabling the precise identification of the temporal characteristics of the pressure waves. By considering  $t_{M,1}$  and  $t_{P,1}$ , the pressure wave speed,  $a$ , is calculated equal to 1172 m/s, in agreement with the geometrical and mechanical characteristics of the SP.

It is important to note that the central value, around which the pressure signals oscillate gradually, slightly decreases in both measurement sections. This phenomenon is attributed to the pressure reduction at the Petrinia piezometric tower, a result of the pump shut-off that supplies it, coupled with the continuous water consumption of the Villaggio del Pescatore and Trieste WDNs, because of the strong interconnection of the supply system described in [2]. Figure 4 shows a magnification of the pressure signal acquired at section M during the first characteristic time. It shows the first increase linked to the maneuver and, therefore, a clear decrease due to the wave reflected by the Petrinia piezometric tower at  $t = 33.69$  s, compatible with the already calculated pressure wave speed. Before this decrease (at  $t = 30.91$  s), a small and abrupt pressure reduction occurs. This reduction could be associated with the number of connections near VP. Due to their proximity and the duration of the maneuver, these connections are indistinguishable. It is noteworthy that, despite the signal becoming noisier over time, three distinct discontinuities, labeled A1, A2, and A3 in Figure 4, and characterized by an "inverted bell" shape, can be discerned in the pressure signal. Indeed, the characteristics of the anomaly nearest to the SDV (namely, A1) inevitably impact the subsequent segments of the pressure signal due to the interactions (both reflections and transmissions) occurring at this anomaly.

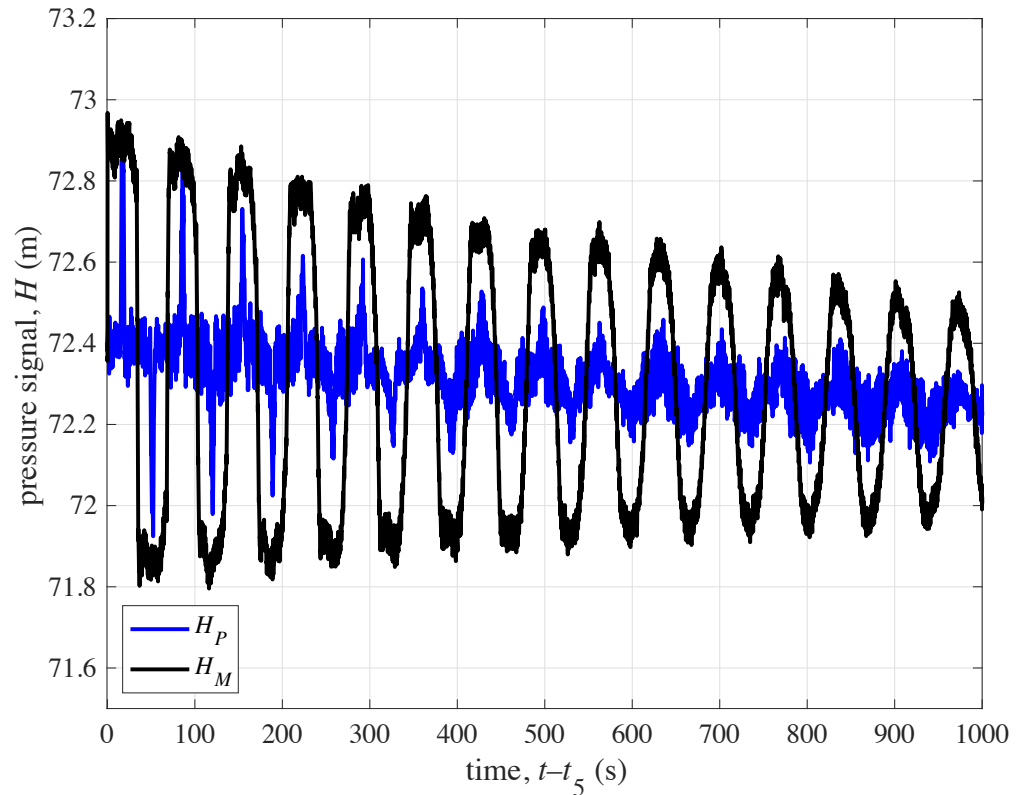


Figure 3. Pressure signals acquired at sections M and P.

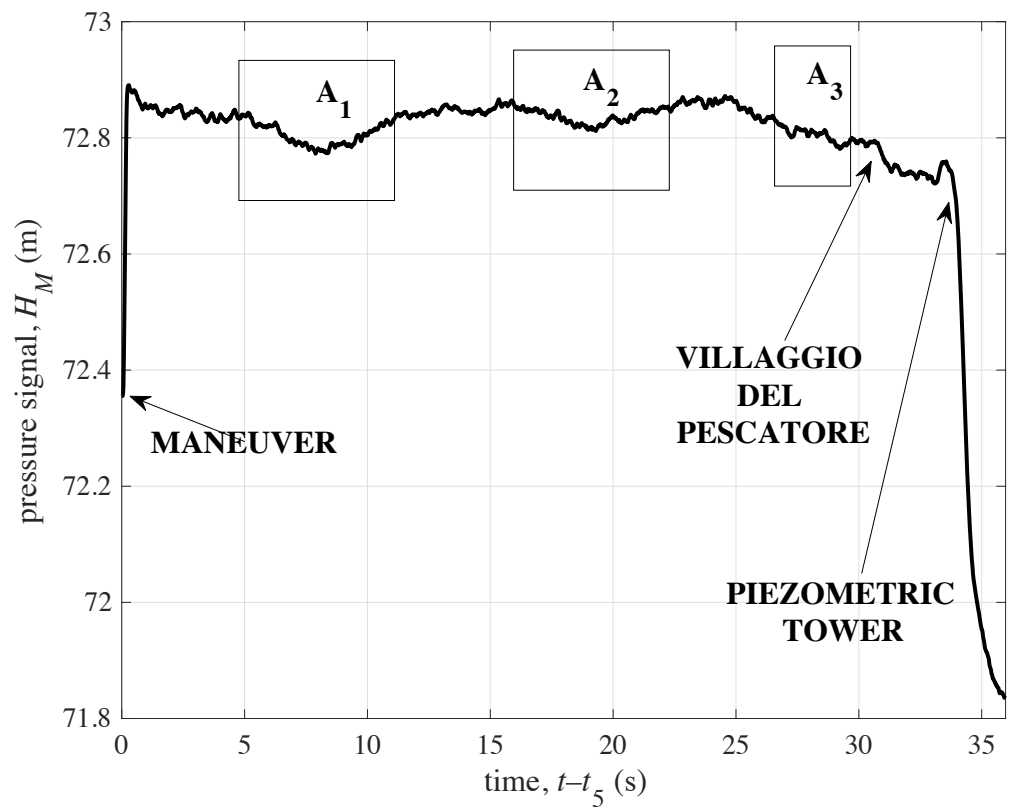


Figure 4. Pressure signal acquired at section M during the first characteristic time.

#### 4. Field Tests Analysis

The analysis of the field test was conducted through a trial-and-error procedure. The hypothesis of air presence within the pipeline was dismissed given the pipeline's

submarine location and the absence of hazardous maneuvers. This assumption is further corroborated by the observed pressure signals at both sections P and M (Figure 3), which exhibit a regular, stable pattern without any spikes, suggesting the absence of air.

The procedure followed is briefly described in Figure 5. Following a detailed analysis of the pressure signals acquired at sections M and P, as well as the evaluation of the pressure wave speed already described, the procedure progresses to include the numerical simulation of the experimental pressure signal. Initially, despite acknowledging the existence of three distinct anomalies, the preliminary phase of this procedure treated the SP as if it were an intact pipeline, incorporating only a branch at Villaggio del Pescatore into the model. The analysis then advanced to a subsequent phase, which opened up considerations for potential pipeline damage. This damage could manifest as a leak, partial wall deterioration, or other types of anomalies, marking a deeper dive into the system’s diagnosis. It is important to highlight that the objective of the numerical simulation is to replicate the key aspects of the transient response accurately. On the contrary, complete concordance between numerical and experimental pressure signals is not expected, nor is it deemed crucial from a management perspective. Inevitable discrepancies arise from uncertainties associated with the physical characteristics of the pipe, such as pipe roughness, the boundary conditions, as well as the noise affecting field data.

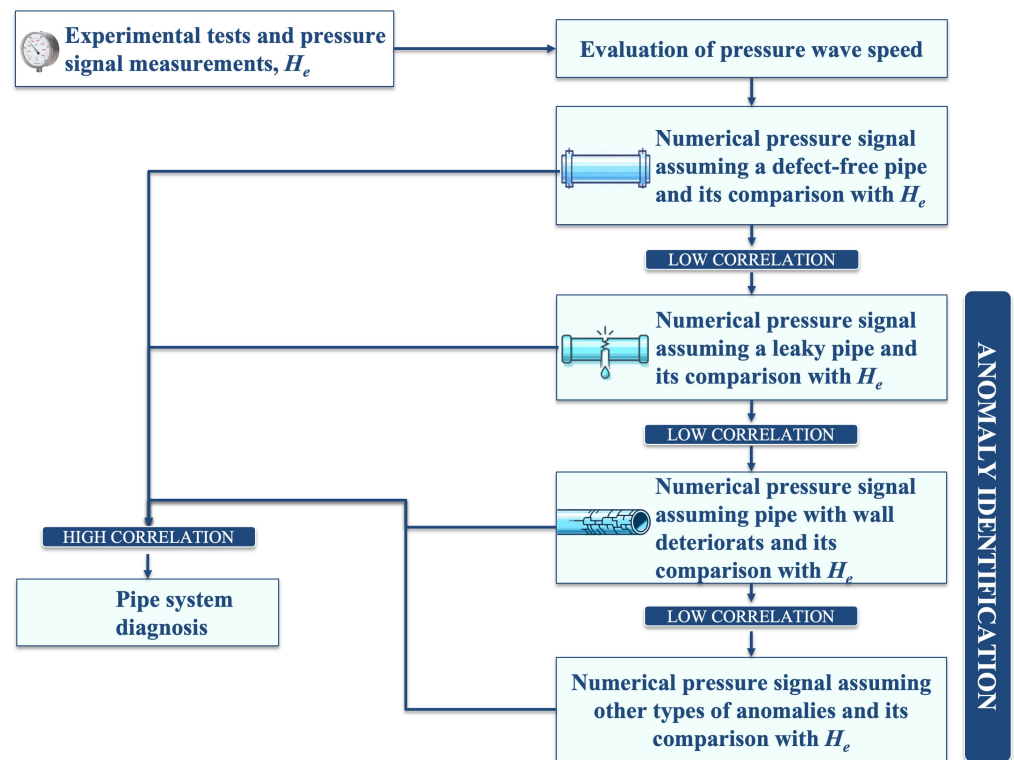
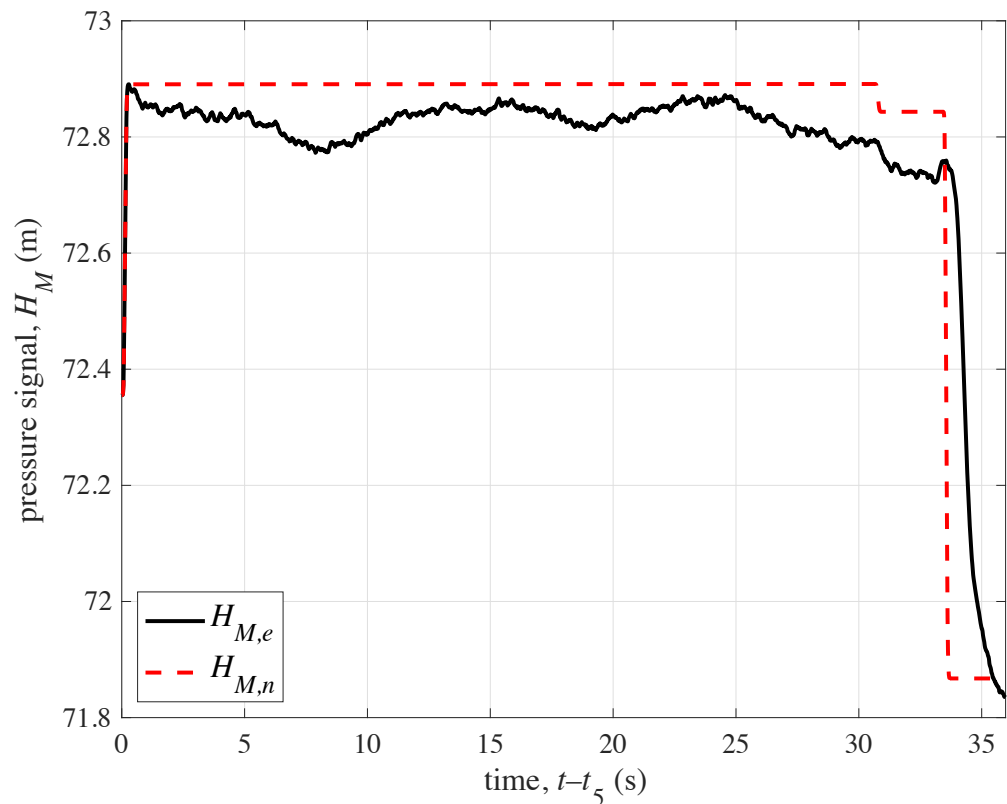


Figure 5. Flow chart illustrating the trial-and-error procedure for diagnosing the pipe system.

Figure 6 shows a comparative analysis between the experimental pressure signal and its numerical counterpart, assuming an intact pipeline; in the figure, the subscripts  $e$  and  $n$  indicate the experimental and numerical values, respectively. The initial increase at  $t = 0$  in the pressure signal is due to the maneuver, while the decrease observed at  $t = 33.69$  s aligns with the expected arrival time of the wave reflected back by the Petrinia piezometric tower. Additionally, a noticeable decrease at  $t = 30.91$  s can be linked to the concentration of connections near VP, as previously discussed. Despite these points of similarity between the numerical and experimental pressure signals, it is evident that the numerical model’s performance is suboptimal. Significant enhancements are required to improve its accuracy. This is particularly evident in the discrepancies observed in Figure 4, where the pressure

variations labeled A1, A2, and A3—encompassing both increases and decreases—are not effectively captured by the numerical model.



**Figure 6.** Comparison of experimental and numerical pressure signals at section M, with the numerical model assuming an intact pipeline.

To identify the nature of the observed anomalies, the working hypothesis initially considered that the first observed pressure reduction might be due to a leak. This assumption led to the determination of the effective leak area,  $A_{L,E}$ , set at  $0.0044 \text{ m}^2$ , as calculated using Equation (11). To test this hypothesis, Figure 7 compares the experimental pressure signal with a numerical simulation incorporating a leak at a distance of about 3.5 km from section M with the specified  $A_{L,E}$  value. It is important to note that the discrepancy in the performance of the numerical simulation indicates that anomaly A1 is unlikely to be a leak. This conclusion is drawn from the observation that the numerical signal does not replicate the increase following the pressure reduction, a feature prominently seen in the experimental data. Considering the insights from Figure 2d and the relevant literature [35], it appears more plausible that this discontinuity could be attributed to wall deterioration rather than a leak. Such a hypothesis is based on the characteristics of the pipe cross-section with one bitumen and three concrete weight coatings (Figure 8), with the relevant thickness indicated as  $S$ .

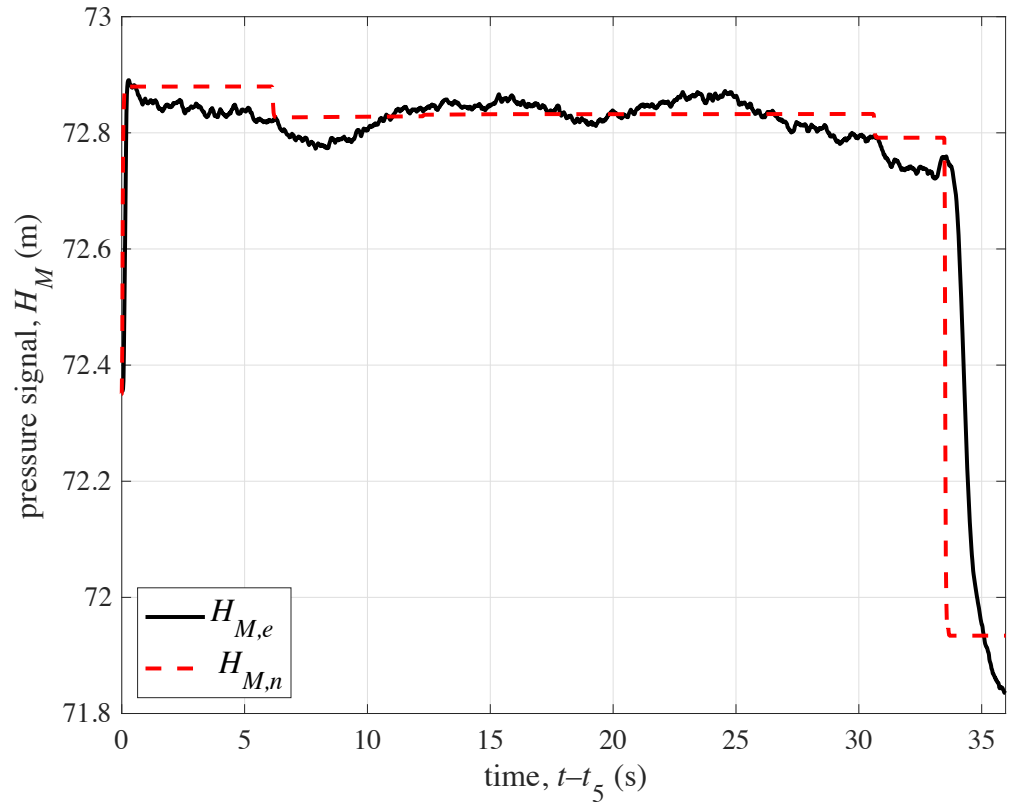


**Figure 7.** Comparison of experimental and numerical pressure signals at section M, with the numerical model assuming a leaky pipeline.

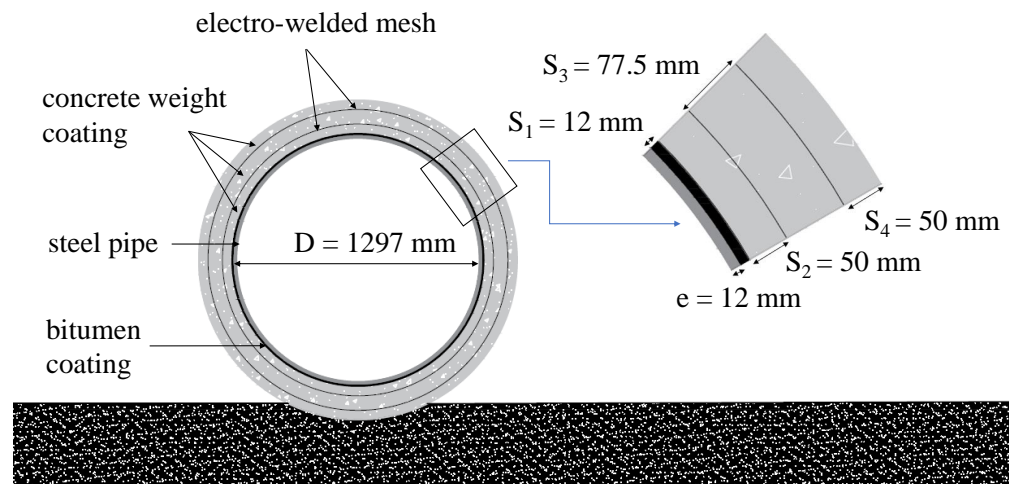


**Figure 8.** Cross-sectional area of the Trieste subsea pipeline.

To accurately represent the characteristics of the identified anomalies, Figure 9 presents the reflection coefficient  $C_{RWD}$  as defined by Equation (12). This involves deriving Young’s modulus of elasticity,  $E$ —assumed to be the same for both the main pipe and the area of partial wall deterioration—from the experimentally measured pressure wave speed ( $a = 1172$  m/s). Figure 9a displays the reflection coefficient for a scenario of partial deterioration of the pipeline’s external lining (coating), with a maintained internal diameter equal to the main pipe ( $D = 1.297$  m). In this case, the pressure wave speed of the deteriorated section,  $a_{WD}$ , in Equation (12) varies as a function of the pipe wall thickness for the specified internal diameter. Conversely, Figure 9b illustrates the reflection coefficient corresponding to an increase in internal diameter due to a reduction in the thickness of the internal wall. In this scenario,  $a_{WD}$  is shown to change depending on both the wall

thickness and adjusted internal diameter of the pipe. The analysis of Figure 9a,b reveals a direct relationship between the severity of wall deterioration and the absolute value of the reflection coefficient. Specifically, the coefficient increases as the wall thickness decreases or as the internal diameter of the pipe enlarges.

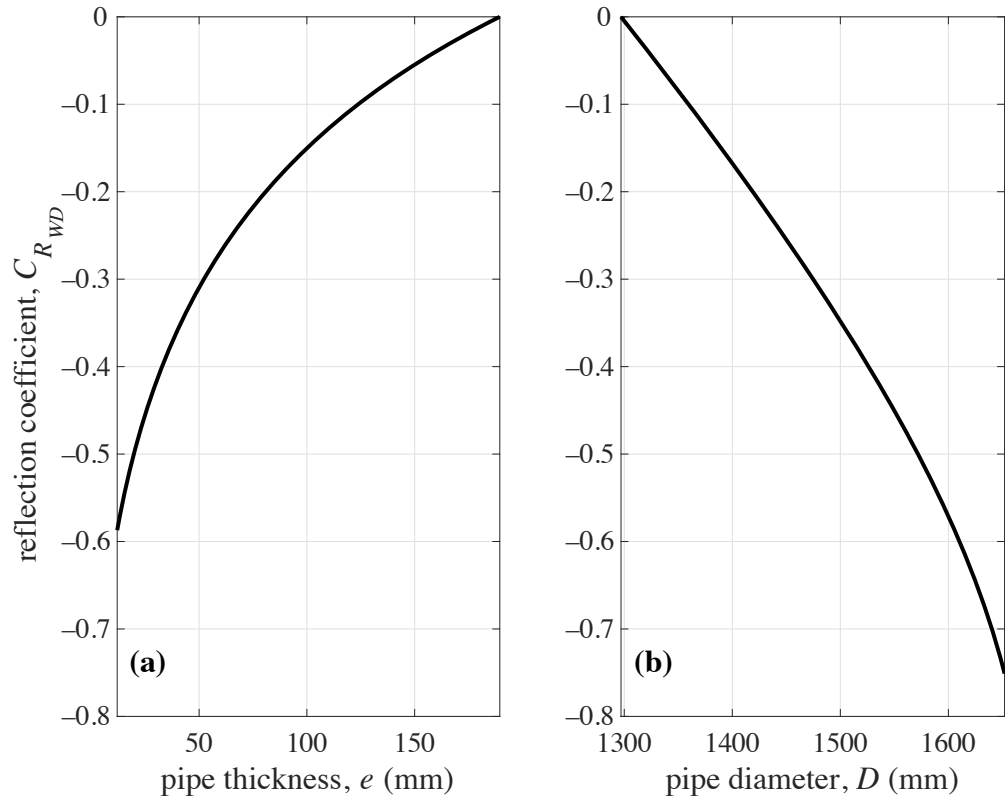


**Figure 9.** Reflection coefficients for wall deterioration vs. (a) the wall thickness, for a partial external lining deterioration with a constant internal diameter, and (b) the internal diameter for reduced internal wall thickness.

It is important to note that the numerical model used in this study was not specifically calibrated or tested for this particular pipeline. As discussed above, the primary objective of the simulation is not to precisely mimic reality, but rather to provide general insights into the types of faults present. Figure 10 illustrates the comparison between experimental and numerical pressure signals at section M, where the numerical model includes considerations for partial wall deterioration. In particular, Figure 10a displays the results for a scenario involving a deteriorated section with a 19.37% reduction in wall thickness and an approximate length of 1.1 km.

The numerical model, while informative, does not precisely align with the experimental pressure signal in the vicinity of anomaly A1. This discrepancy suggests that the onset of deterioration might occur 600 m earlier than initially thought and progresses gradually. Figure 10b explores this hypothesis by illustrating the impact of adding a deteriorated section. This section, characterized by a 9% reduction in wall thickness, is considered to begin approximately 600 m before the previously identified deteriorated section, thereby extending the area of potential wall degradation.

As shown in Figure 10b, the subsequent anomaly, labeled A2, cannot be attributed to the same deteriorated section identified in A1. As a result, an alternative hypothesis was explored. Initially, anomaly A2 was presumed to be a leak. However, similar to the case with A1, the results from this assumption (not depicted here) were unsatisfactory. Therefore, it was equivalently hypothesized that A2 might also be the result of another wall deterioration. Figure 10c illustrates the effects of introducing an additional deteriorated

section into the model at about 9 km from section M. This section is characterized by an 18% reduction in wall thickness and extends over an approximate length of 1.7 km.

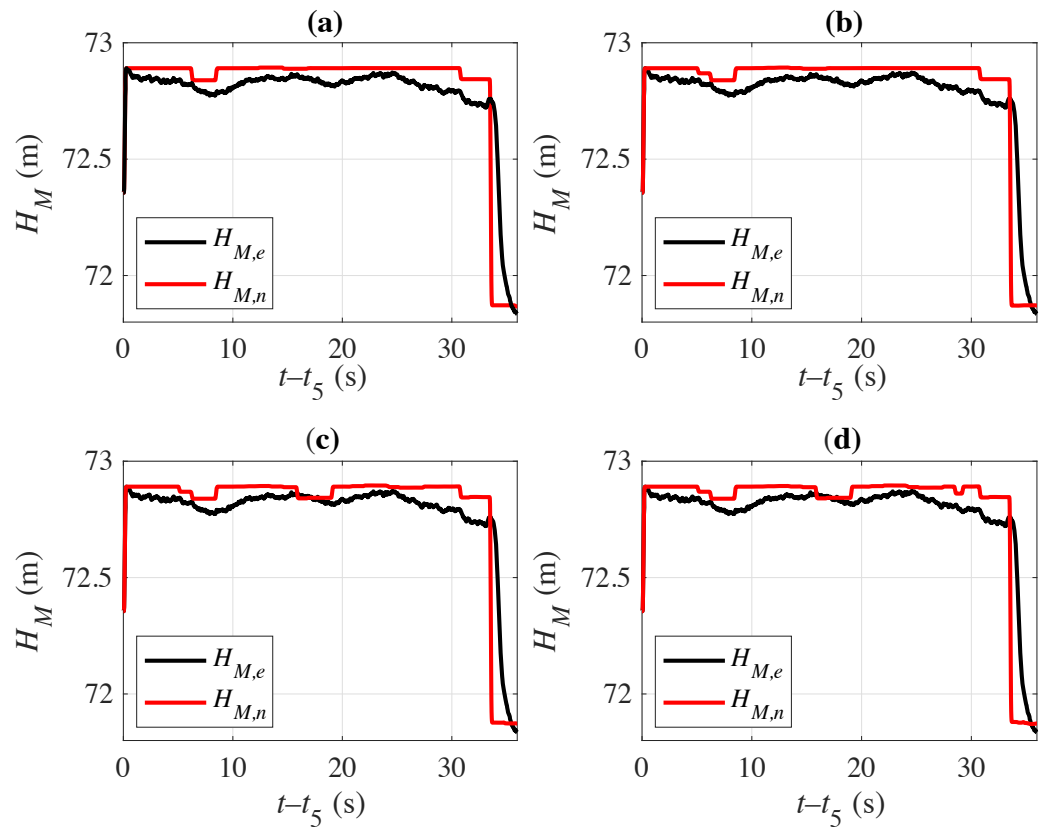


**Figure 10.** Comparison of experimental and numerical pressure signals at section M, with the numerical model incorporating assumptions of partial wall deterioration.

Figure 10c reveals that the anomaly labeled A3 is distinct from the deteriorated sections identified as A1 and A2. Consequently, it was hypothesized that A3 might similarly be a result of additional wall deterioration. Figure 10d depicts the introduction of another deteriorated section into the model, positioned approximately 16.3 km from section M. This section is defined by a 12% reduction in wall thickness and spans an approximate length of 0.4 km, further illustrating the complexity and variability of deterioration within the pipeline.

The results derived from the proposed method were reported to AceGasApsAmga SpA, which manages the SP. The company’s technicians had already considered the possibility of such wall deteriorations, associating them with the submarine landslide of 1980 that led to partial silting and displacement of a segment of the SP. Diver inspections highlighted substantial deterioration of the external wall and concrete coating in section A3, as shown in Figure 11.

During inspections of other sections, limited visibility—despite the use of high-intensity lighting—prevented a definitive assessment of external wall condition, leaving the potential for undetected deterioration. Importantly, these observations do not rule out the presence of internal wall deterioration, which remains a consideration for comprehensive structural integrity evaluation.



**Figure 11.** External wall deterioration located in Section A3 (it is worth noting that the poor resolution of the image is due to the peculiarity of the subsea environment).

## 5. Conclusions

This paper, the second in a series of two companion papers, discusses the results of the transient field tests carried out for fault detection in the Trieste subsea pipeline managed by AcegasApsAmga SpA (Hera Group). In particular, the numerical and analytical models used to analyze the pressure signals acquired during the transient tests are presented. The first paper discusses and justifies, as a necessary premise, all the actions carried out to prepare the tests and to place the SP in the most appropriate flow conditions. The procedure used, agreed in all details with the water company's technicians, did not cause any problems and can be repeated at any time. In particular, users have not noted any shortfall in supply, either in terms of discharge or pressure. This gives the company's technicians complete autonomy and guarantees minimum costs.

The transient numerical model has been used within a trial-and-error procedure, highlighting the effect of possible anomalies by comparing the numerical results with the acquired pressure signals. In particular, it has been shown that the insertion of a small pressure wave (i.e., with an amplitude of about 0.60 m) has highlighted sections of the subsea pipeline characterized by wall deterioration.

The results of the proposed method are substantially corroborated by the diver inspection, which essentially confirms some wall deterioration of the concrete coating in the highlighted sections of the subsea pipelines.

**Author Contributions:** Conceptualization, S.M., C.C., B.B., L.T. and A.R.; methodology, S.M., C.C., B.B., L.T. and A.R.; software, S.M., C.C. and B.B.; validation, S.M., C.C., B.B., L.T., A.R. and M.C.; formal analysis, S.M., C.C., B.B., L.T., A.R. and M.C.; investigation, S.M., C.C., B.B., L.T., A.R. and M.C.; resources, S.M., C.C. and B.B.; data curation, S.M., C.C., B.B., L.T., A.R. and M.C.; writing—original draft preparation, S.M., C.C. and B.B.; writing—review and editing, S.M., C.C., B.B., L.T., A.R. and M.C.; project administration, S.M., C.C. and B.B.; funding acquisition, S.M., C.C. and B.B. All authors have read and agreed to the published version of the manuscript.

**Funding:** This research was funded by the University of Perugia *Fondo di ricerca di Ateneo-edizioni 2021 e 2022*, and the Ministry of University and Research (MUR) under the Project of Relevant Interest—PRIN2022—“Hybrid Transient-machine learning approach for ANomaly DEtection and classification in water transmission Mains (TANDEM)” (CUP: J53D23002110006).

**Institutional Review Board Statement:** Not applicable.

**Informed Consent Statement:** Not applicable.

**Data Availability Statement:** Experimental pressure signals are available upon request.

**Acknowledgments:** This research has been executed within a joint project between the Department of Civil and Environmental Engineering (DICA) of the University of Perugia and AcegasApsAmga SpA, Padua, Italy. The support of Filomena Maietta and C. Del Principe of DICA and AcegasApsAmga SpA technicians within the field activity is highly appreciated.

**Conflicts of Interest:** Lorenzo Tirello and Andrea Rubin were employed by AcegasApsAmga SpA. The remaining authors declare that the research was conducted in the absence of any commercial or financial relationships that could be construed as a potential conflict of interest.

## References

- Laven, L.; Lambert, A.O. What do we know about real losses on transmission mains? In Proceedings of the IWA Specialised Conference “Water Loss 2012”, Manila, Philippines, 26–29 February 2012.
- Meniconi, S.; Brunone, B.; Tirello, L.; Rubin, A.; Cifrodelli, M.; Capponi, C. Transient tests for checking the Trieste subsea pipeline: Towards the field tests. *J. Mar. Sci. Eng.* **2024**, *12*, 374. [[CrossRef](#)]
- Ho, M.; El-Borgh, S.; Patil, D.; Song, G. Inspection and monitoring systems subsea pipelines: A review paper. *Struct. Health Monit.* **2020**, *19*, 606–645. [[CrossRef](#)]
- Amaechi, C.V.; Hosie, G.; Reda, A. Review on subsea pipeline integrity management: An operator’s perspective. *Energies* **2022**, *16*, 98. [[CrossRef](#)]
- Cawley, P.; Lowe, M.; Alleyne, D.; Pavlakovic, B.; Wilcox, P. Practical long range guided wave testing: Applications to pipes and rail. *Mater. Eval.* **2003**, *61*, 66–74.
- Gazis, D.C. Three-dimensional investigation of the propagation of waves in hollow circular cylinders. 1. Analytical foundation. *J. Acoust. Soc. Am.* **1959**, *31*, 568573. [[CrossRef](#)]
- Reda, A.; Shahin, M.A.; Sultan, I.A.; Amaechi, C.V.; McKee, K.K. Necessity and suitability of in-line inspection for corrosion resistant alloy (CRA) clad pipelines. *Ships Offshore Struct.* **2023**, *18*, 1360–1366. [[CrossRef](#)]
- Kazeminasab, S.; Sadeghi, N.; Janfaza, V.; Razavi, M.; Ziyadidegan, S.; Banks, M.K. Localization, mapping, navigation, and inspection methods in in-pipe robots: A review. *IEEE Access* **2021**, *9*, 162035–162058. [[CrossRef](#)]
- Taghvaei, M.; Beck, S.B.M.; Boxall, J.B. Leak detection in pipes using induced water hammer pulses and cepstrum analysis. *Int. J. COMADEM* **2010**, *13*, 19–25.
- Alawadhi, A.; Tartakovsky, D.M. Bayesian update and method of distributions: Application to leak detection in transmission mains. *Water Resour. Res.* **2020**, *56*, e2019WR025879. [[CrossRef](#)]
- Brunone, B.; Maietta, F.; Capponi, C.; Keramat, A.; Meniconi, S. A review of physical experiments for leak detection in water pipes through transient tests for addressing future research. *J. Hydraul. Res.* **2022**, *60*, 894–906. [[CrossRef](#)]
- Contractor, D. The reflection of waterhammer pressure waves from minor losses. *J. Basic Eng.* **1965**, *87*, 445–451. [[CrossRef](#)]
- Mohapatra, P.; Chaudhry, M.; Kassem, A.; Moloo, J. Detection of partial blockage in single pipelines. *J. Hydraul. Eng.* **2006**, *132*, 200–206. [[CrossRef](#)]
- Sattar, A.M.; Chaudhry, M.H.; Kassem, A.A. Partial blockage detection in pipelines by frequency response method. *J. Hydraul. Eng.* **2008**, *134*, 76–89. [[CrossRef](#)]

15. Wang, X.; Lin, J.; Keramat, A.; Ghidaoui, M.S.; Meniconi, S.; Brunone, B. Matched-field processing for leak localization in a viscoelastic pipe: An experimental study. *Mech. Syst. Signal Process.* **2019**, *124*, 459–478. [[CrossRef](#)]
16. Brunone, B.; Maietta, F.; Capponi, C.; Duan, H.F.; Meniconi, S. Detection of partial blockages in pressurized pipes by transient tests: A review of the physical experiments. *Fluids* **2023**, *8*, 19. [[CrossRef](#)]
17. Duan, H.F.; Lee, P.J.; Kashima, A.; Lu, J.; Ghidaoui, M.S.; Tung, Y.K. Extended blockage detection in pipes using the system frequency response: Analytical analysis and experimental verification. *J. Hydraul. Eng.* **2013**, *139*, 763–771. [[CrossRef](#)]
18. Duan, H.F.; Lee, P.J.; Ghidaoui, M.S.; Tuck, J. Transient wave-blockage interaction and extended blockage detection in elastic water pipelines. *J. Fluids Struct.* **2014**, *46*, 2–16. [[CrossRef](#)]
19. Gong, J.; Lambert, M.F.; Nguyen, S.T.N.; Zecchin, A.; Simpson, A.R. Detecting thinner-walled pipe sections using a spark transient pressure wave generator. *J. Hydraul. Eng.* **2018**, *144*, 06017027. [[CrossRef](#)]
20. Liggett, J.A.; Chen, L.C. Inverse transient analysis in pipe networks. *J. Hydraul. Eng.* **1994**, *120*, 934–955. [[CrossRef](#)]
21. Colombo, A.; Lee, P.; Karney, B.W. A selective literature review of transient-based leak detection methods. *J. Hydro-Environ. Res.* **2009**, *2*, 212–227. [[CrossRef](#)]
22. Xu, X.; Karney, B. An overview of transient fault detection techniques. In *Modeling and Monitoring of Pipelines and Networks*; Springer: Cham, Switzerland, 2017; pp. 13–37.
23. Ayati, A.H.; Haghighi, A.; Lee, P.J. Statistical review of major standpoints in hydraulic transient-based leak detection. *J. Hydraul. Struct.* **2019**, *5*, 1–26.
24. Che, T.C.; Duan, H.F.; Lee, P.J. Transient wave-based methods for anomaly detection in fluid pipes: A review. *Mech. Syst. Signal Process.* **2021**, *160*, 107874. [[CrossRef](#)]
25. Capponi, C.; Martins, N.M.; Covas, D.I.C.; Brunone, B.; Meniconi, S. Transient test-based techniques for checking the sealing of in-line shut-off valves and capturing the effect of series junctions—Field tests in a real pipe system. *Water* **2024**, *16*, 3. [[CrossRef](#)]
26. Duan, H.; Pan, B.; Wang, M.; Chen, L.; Zheng, F.; Zhang, Y. State-of-the-art review on the transient flow modeling and utilization for urban water supply system (UWSS) management. *J. Water Supply Res. Technol.-AQUA* **2020**, *69*, 858–893. [[CrossRef](#)]
27. Covas, D.; Ramos, H. Case studies of leak detection and location in water pipe systems by inverse transient analysis. *J. Water Resour. Plan. Manag.* **2010**, *136*, 248–257. [[CrossRef](#)]
28. Pickering, D.; Park, J.M.; Bannister, D.H. *Utility Mapping and Record Keeping for Infrastructure*; The World Bank: Washington, DC, USA, 1993; p. 69.
29. Costello, S.; Chapman, D.; Rogers, C.; Metje, N. Underground asset location and condition assessment technologies. *Tunn. Undergr. Space Technol.* **2007**, *22*, 524–542. [[CrossRef](#)]
30. King, M.; Shemirami, S. *Smart Infrastructure: Mapping Underground Utilities*; KPMG Int. Cooperative: Amstelveen, The Netherlands, 2017; p. 12.
31. Capponi, C.; Meniconi, S.; Lee, P.J.; Brunone, B.; Cifrodelli, M. Time-domain analysis of laboratory experiments on the transient pressure damping in a leaky polymeric pipe. *Water Resour. Manag.* **2020**, *34*, 501–514. [[CrossRef](#)]
32. Bohorquez, J.; Simpson, A.R.; Lambert, M.F.; Alexander, B. Merging fluid transient waves and artificial neural networks for burst detection and identification in pipelines. *J. Water Resour. Plan. Manag.* **2021**, *147*, 4020097. [[CrossRef](#)]
33. Ayati, A.H.; Haghighi, A.; Ghafouri, H.R. Machine learning-assisted model for leak detection in water distribution networks using hydraulic transient flows. *J. Water Resour. Plan. Manag.* **2022**, *148*, 4021104. [[CrossRef](#)]
34. Bohorquez, J.; Lambert, M.F.; Alexander, B.; Simpson, A.R.; Abbott, D. Stochastic Resonance Enhancement for Leak Detection in Pipelines Using Fluid Transients and Convolutional Neural Networks. *J. Water Resour. Plan. Manag.* **2022**, *148*, 4022001. [[CrossRef](#)]
35. Gong, J.; Lambert, M.F.; Simpson, A.R.; Zecchin, A.C. Detection of localized deterioration distributed along single pipelines by reconstructive MOC analysis. *J. Hydraul. Eng.* **2014**, *140*, 190–198. [[CrossRef](#)]
36. Wylie, E.; Streeter, V. *Fluid Transients in Systems*; Prentice-Hall Inc.: Hoboken, NJ, USA, 1993; p. 463.
37. Chaudhry, M.H. *Applied Hydraulic Transients*, 3rd ed.; Springer: New York, NY, USA, 2014; p. 583.
38. Swaffield, J.; Boldy, A. *Pressure Surges in Pipe and Duct Systems*; Ashgate Publishing Group: Farnham, UK, 1993; p. 380.
39. Pan, B.; Duan, H.F.; Meniconi, S.; Urbanowicz, K.; Che, T.C.; Brunone, B. Multistage frequency-domain transient-based method for the analysis of viscoelastic parameters of plastic pipes. *J. Hydraul. Eng.* **2020**, *146*, 04019068. [[CrossRef](#)]
40. Pezzinga, G. Evaluation of unsteady flow resistances by quasi-2D or 1D models. *J. Hydraul. Eng.* **2000**, *126*, 778–785. [[CrossRef](#)]
41. Brunone, B.; Golia, U.M. Discussion of “Systematic evaluation of one-dimensional unsteady friction models in simple pipelines” by J.P. Vitkovsky, A. Bergant, A.R. Simpson, and M.F. Lambert. *J. Hydraul. Eng.* **2008**, *134*, 282–284. [[CrossRef](#)]
42. Liou, C. Pipeline leak detection by impulse response extraction. *J. Fluids Eng.* **1998**, *120*, 833–838. [[CrossRef](#)]

**Disclaimer/Publisher’s Note:** The statements, opinions and data contained in all publications are solely those of the individual author(s) and contributor(s) and not of MDPI and/or the editor(s). MDPI and/or the editor(s) disclaim responsibility for any injury to people or property resulting from any ideas, methods, instructions or products referred to in the content.